Comparison of surface IR radiometer and near surface air temperatures over a grass covered field

by John Schieldge, Jet Propulsion Laboratory, Pasadena, CA

Introduction

A number of approaches for estimating the surface sensible (H) and latent heat (LE) flux densities from satellite remote sensing measurements make use of the following expressions:

(1) $H = -\rho C_p(T_{rad} - T_{air})/r_H$

(2) $LE = R_n - G - H$,

where ρ is the air density, C_p the specific heat of air at constant pressure, T_{rad} is the radiometric temperature of the surface as measured in the thermal infrared portion of the electromagnetic spectrum, T_{air} is the air temperature measured at some height (z) above the ground (e.g. 2-m), R_n is the net radiative heat flux density, G is the soil heat flux density, and r_H is the resistance to heat transfer between the surface and z. Equation (2) is the surface energy balance rewritten so that LE is calculated as the residual term after R_n, H, and G have been calculated. G is often calculated as some constant proportional to R_n. R_n can be estimated from satellite remote sensing data at visible and infrared wavelengths (Sellers et al, 1990). Estimation of R_n, and then G, in this way results in an uncertainty in their values of 20 % or more.

There are a number of other factors that confound the calculation of H and LE from (1) and (2), and these have been reviewed in the current literature (Kustas and Norman, 1996). These factors include the assumption that the calculation of H is appropriately done through the use of Monin-Obukhov Similarity Theory /MOST (Kaimal and Finnegan, 1994) which implies uniformity of surface conditons . Furthermore, the resistance to heat transfer is affected by wind speed, surface roughness, and atmospheric stability in a complicated and non-linear way, and is not easily estimated from remote sensing, and supporting meteorological, data.

Above and beyond these factors, which have been extensively studied and commented upon in the literature, are several fundamental issues that have to do with the suitability of the use of the measured variables in (1) and (2). One important issue is: if T_{rad} varies with instrument viewing angle, what value of T_{rad} is to be used in (1)?

In this paper, we shall not concern ourselves with any of the issues mentioned above, but instead we will concentrate on two other fundamental measurement issues. The first issue is the appropriateness of calculating the difference T_{rad} and T_{air}. T_{rad} is essentially an instantaneous measurement taken from the satellite fly over. T_{air} is typically an average of the air temperature over a period of one-half to one hour. The second issue is what percentage of the variance in T_{rad} is contributed by turbulent air (inactive) eddies that do not share in the process of transporting heat upward from the surface? From MOST, use of equation (1) implies that T_{rad} is produced exclusively from active eddies that transport energy upward from the surface.

We explore these two issues using a data set collected in the Duke University forest near Durham, North Carolina during August and September of 1996. The data consists of surface radiometric and air temperature measurements made over a 6 week period.

Method of Analysis

The methodology used in this study is described in Katul et al (1997). Principally, it consists of an analysis of the wind speed, air temperature, and surface radiometeric temperature from a set of instruments mounted at a height of about 3-m (see below). The analysis consists of a spectral decomposition of the wind and temperature data using orthonormal wavelet transforms. The particular basis function for this analysis is the Haar function which is an odd rectangular pulse pair and one of the earliest and simplest types of orthonormal wavelets (Haar, 1955). Use of wavelet transforms over Fourier transforms is an advantage in this case because the turbulent kinetic energy can be partitioned into just a few wavelet coefficients, thus facilitating the analysis on the effects of inactive eddies on the variance of T_{rad}.

Data Collection

The data was collected in the Duke University forest near Durham, North Carolina from about the middle of August until the last week of September 1996. The site was a dense grass covered field about 400-m square and surrounded on all sides by trees whose height was about 13-m. The average height of the grass was 1-m. At about 200-m from the northern edge of the field , we mounted a suite of instruments over a height range of 2 to 4-m. A Gill 3-axis sonic anemometer was mounted at a height of 3.75-m and an Everest Infrared Radiometer (IRR) was mounted nearby at a height of 3.1-m. The IRR was mounted facing north and at an angle of 75° from the vertical. (An angle of 0° is looking down and 90° is looking parallel to the ground). The field of view of the IRR was 15°. The sonic anemometer was used to measure the two horizontal (u,v) and the vertical (w) components of the wind as well as the air Temperature (T_{air}) . T_{air} was derived from the speed of sound computed from the sonic measurements, and verified by comparing the results with those from a fine wire thermocouple (12 micron diameter wire) mounted about 10 cm away from the center of the sonic 3-axis transducer configuration. The IRR was used to measure the surface radiometric brightness temperature . Additional data was collected in and above the grass canopy from a vertical array of 9 fine wire thermocouples at heights of 0.0, 0.2, 0.3,0.6,0.8,1.2,1.8,2.5, and 3.1-m.

The data were sampled at 5 Hz and recorded on a 21 X Campbell Scientific datalogger. The data to be used in the wavelet analysis were divided into segments of 2^{13} (= 8192) data points corresponding to approximately 27 minute intervals. All other data were divided into 20 minute segments.
An emissivity of 0.95 for grass (Garratt, 1992) was used to convert the surface radiometric brightness temperature to the kinematic temperature of the grass. Due to the density of the grass and the viewing angle of the IRR it is likely that only the top third of the grass canopy was viewed and none of the soil was in the IRR field of view. The data that we collected pertained to cloud free days from about 0900 to 1700 LT. During the data collection period the soil moisture content remained high due to frequent passage near, and occasionally over, the site by a number of hurricanes and tropical storms. In fact September 1996 was the wettest month ever recorded in the history of North Carolina weather. This ensured that the evapotranspiration was atmosphere limited and not soil limited.

Results

Figure 1 shows the time trace of the IRR surface temperature for a 20 minute interval on the morning of September 18. The data have been detrended and the mean value subtracted from the data. This illustrates the problem of using a near instantaneous remotely sensed estimate of temperature. While the air temperature (T_{air}) in (1) is usually averaged over 20 to 60 minutes , the appropriate value of T_{rad} is not so evident and , in this case, can be up to 6 degrees different from one part of the record to another. This could result in errors in H of 100% or more depending upon what time the T_{rad} observation were made. Of course, T_{rad} is usually not calculated from a single pixel (and Figure 1 shows why this is not a good idea) but from an average of a number of neighboring pixels surrounding the coordinates of interest. Taylor's (1938) "frozen flux" theorem is usually invoked and it is assumed that the pixels upstream along the direction of the prevailing winds are advected over the site of interest without changing their properties, i.e.

the turbulence characteristics are "frozen into" the wind flow. Therefore, one can trace back in time what pixel upstream contributed to the turbulent flux densities at a specific location, and then can use that set of pixels appropriate to the 20-60 minute average of T_{air}. Theoretically, we have a time averaged value of T_{rad} from a spatial average of T_{rad} derived from the image. This allows the T_{rad} and T_{air} measurements to be more synchronous than in the case where an instantaneous value of T_{rad} is used with a time averaged value of T_{air}. This requires some knowledge of the wind vectors over a region and this data is not always available in any detail. So this makes the number and location of pixels to be used to average T_{rad} a problematical issue most of the time, and further research needs to be done in this area in terms of the appropriate averaging to do.

Figure 2 shows the correlation of the fine wire thermocouple (fwtc) air measurements with the IRR surface temperature measurements made at 9 heights above the ground . Five fwtcs were located inside the grass canopy (these are labled tc1 through tc5) and four above the canopy (labled fwtc1 through fwtc4). The cross-correlations were done by Fourier transform of the data. The fwtc data above the grass canopy show very little correlation with the IRR data, most correlations being less than 0.3. The correlations of fwtc measurements made inside the grass canopy are fairly good with the best correlations (~0.9) being in the upper third of the canopy. This confirms the assumption stated earlier that due to the viewing angle (75° from vertical) most of the radiative energy collected by the IRR comes from the upper layers of the canopy.

Figures 3 and 4 show the results of the wavelet analysis. In these figures T_{rad} is denoted by T_s. Figure 3 is the total wavelet energy (KE_{Ts}) of the radiometric surface temperature normalized by the variance ($\sigma_{Ts}\,\sigma_{Ts}$) of T_s. The figure is a plot of KE_{Ts} versus wavenumber ($= 2\pi/L$) where L is the characteristic scale length of the turbulence in the boundary layer. The vertical bar in the figure indicates the peak of the energy as a function of the scale size of the turbulent eddies. The bar position corresponds to an eddy size of about 1200-m which is on the order of the vertical extent of the atmospheric boundary for the clear days used in the study. This implies that the driving force behind the surface fluctuations in T_s (T_{rad}) are due to the effects of large scale inactive eddies. Near the surface such large eddies do not contribute much to the upward transport of heat because their fluctuations (and corresponding air motions) are nearly parallel to the ground at these heights. This effect is also shown in the total wavelet energy of the covariance of longitudinal winds speed (u) and Ts in Figure 4. The interaction between the ground level wind speeds and the surface radiometric temperature indicates that the maximum effect is also at about 1200-m. We also computed correlations between the u and T_s data sets and found values up to -0.7. All these results indicate that inactive eddies can contribute to a significant part of the signal from a surface viewed by an infrared radiometer.

Summary and Conclusions

First, equations (1) and (2) are often used to estimate H and LE from a combination of remotely sensed data (including T_{rad}) and ancillary in situ ground meteorological data. This combination creates a mismatch of scales since remote sensing data is spatially extensive and temporally limited while the converse is true of ground in situ measurements. Since H depends upon the difference between T_{rad} and T_{air}, it is important to try and match the temporal and spatial scales as much as possible. Further research in this area needs to be done to limit the uncertainty in H and LE calculations due to this effect.

Second, fluctuations in T_{rad} can be caused by the large scale motions of "big eddies" whose size is comparable to the thickness (1-3 km) of the daytime atmospheric boundary layer. These eddies do not contribute significantly to the vertical transport of heat and moisture near the surface. This might involve some adjustment in the calculation of H and LE from remotely sensed data.

List of References

Garratt, J. (1992). *The Atmospheric Boundary Layer*. Cambridge University Press, Cambridge.

Haar, A. (1955). Zur theorie der Orthogonalen Funktionen-System. *Math Annalen* 5, 17 - 31.

Kaimal, J. and Finnigan, J. (1994). *Atmospheric Boundary Layer Flows*, Oxford University Press, New York.

Katul, G., Schieldge, J., Kuhn,G., Hsieh, C.-I, Vidakovic,B., (1997). Skin temperature perturbations induced by surface layer turbulence. Submitted to *Water Resour. Res.*

Kustas, W. and Norman, J. (1996). Use of remote sensing for evapotranspiration monitoring over land. *Hydrological Sciences* 41, 495 - 516.

Sellers,P. Rasool,,S.,Bolle,H. (1990). A review of satellite data algorithms for studies of the land surface. *Bull. Amer. Meteorol. Soc.* 71, 1429 - 1447.

Taylor, G. (1938). The spectrum of turbulence. *Proc. Roy. Soc. A*. CLXIV, 476 - 490.

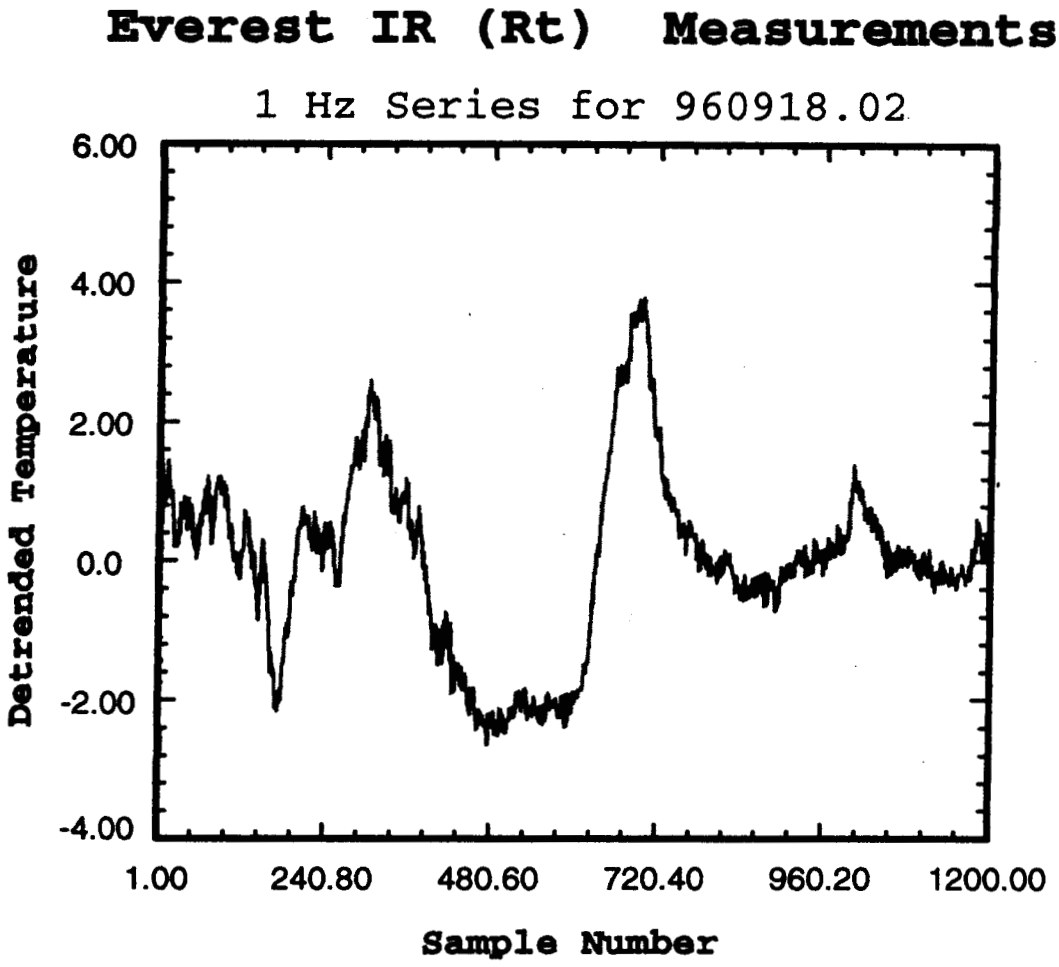
Everest IR (Rt) Measurements
1 Hz Series for 960918.02
Detrended Temperature
6.00
4.00
2.00
0.0
-2.00
-4.00
1.00
240.80
480.60
720.40
960.20
1200.00
Sample Number

Correlations of TC Mast Data

9 levels from FFT Method on t960918.02

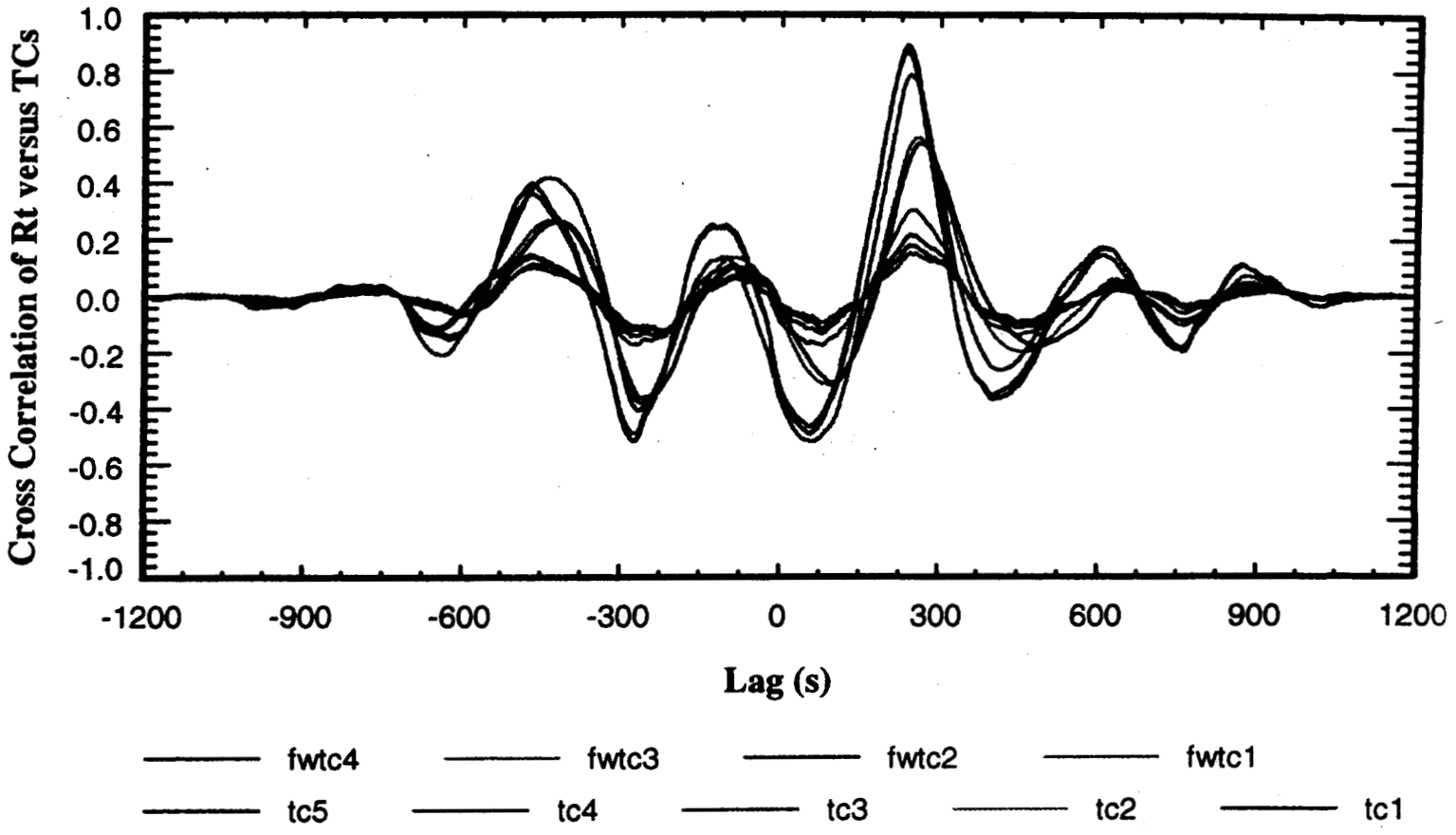

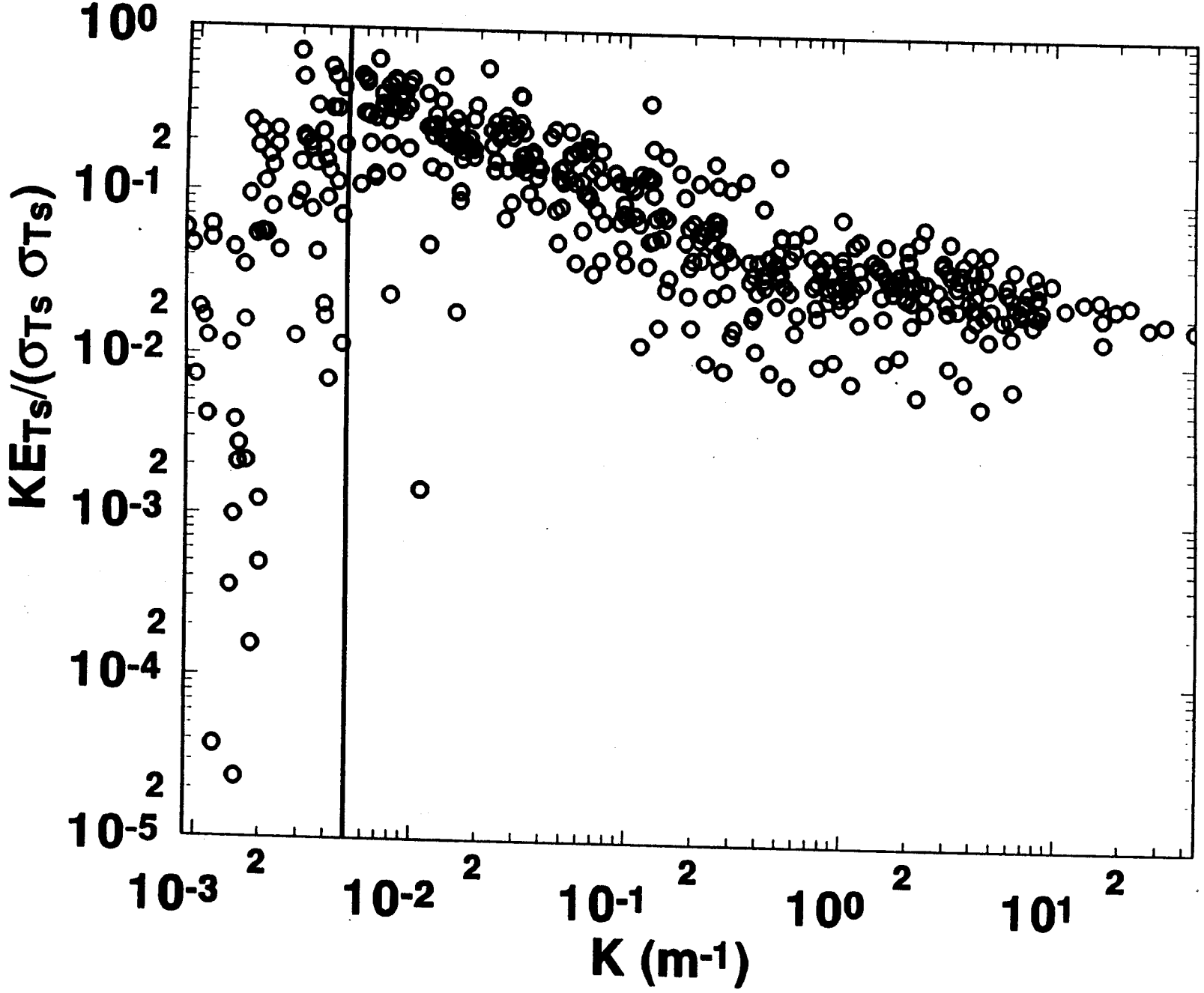
10^0
10^{-1}
10^{-2}
10^{-3}
10^{-4}
10^{-5}
$KE_{Ts}/(\sigma_{Ts}\,\sigma_{Ts})$
10^{-3}
10^{-2}
10^{-1}
10^0
10^1
K (m^{-1})

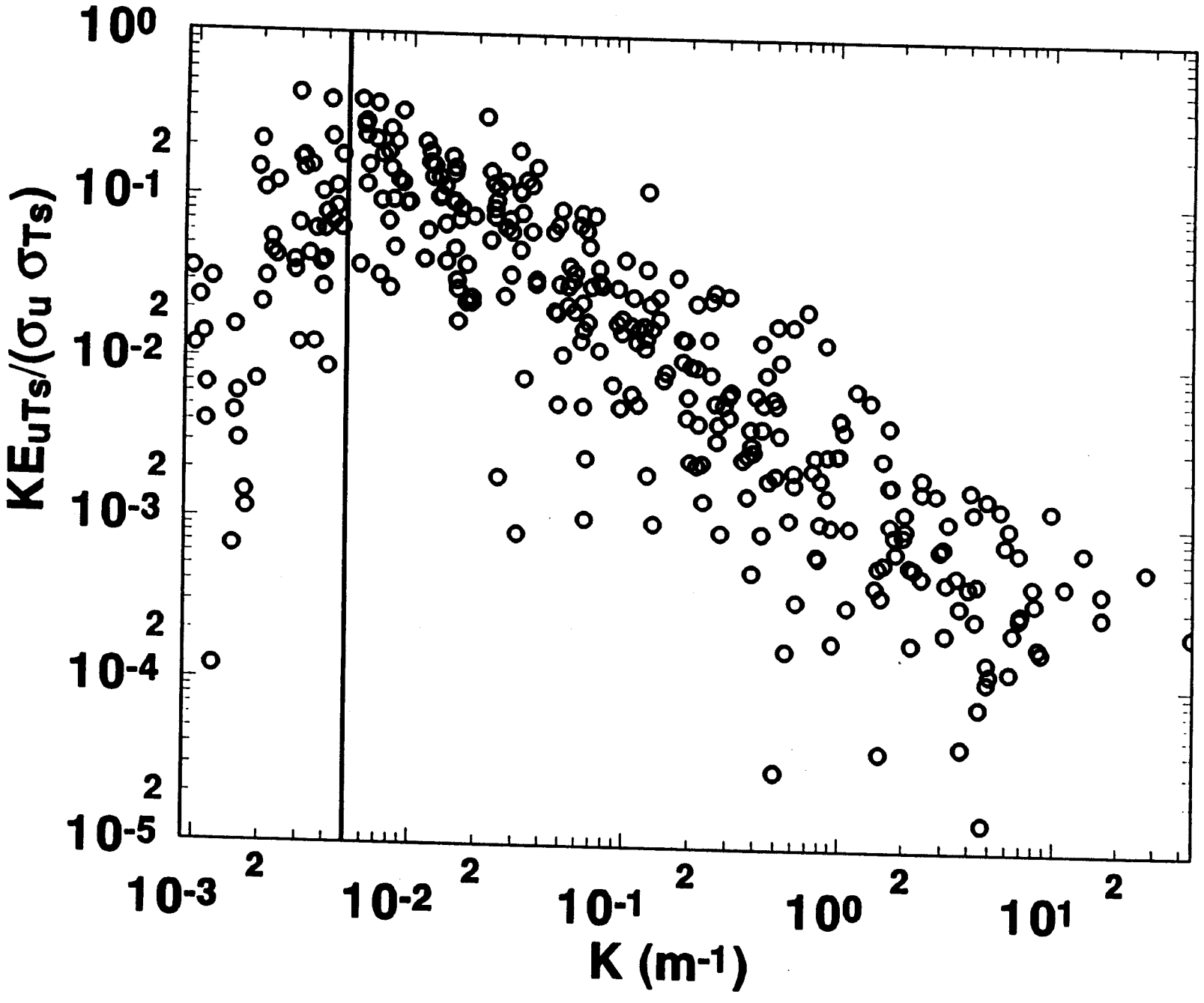
10^0
10^{-1}
10^{-2}
10^{-3}
10^{-4}
10^{-5}
$KE_{uTs}/(\sigma_u \sigma_{Ts})$
10^{-3}
10^{-2}
10^{-1}
10^0
10^1
K (m^{-1})